ChemComm

COMMUNICATION

View Article Online
View Journal | View Issue

Cite this: *Chem. Commun.*, 2024, **60**, 1039

Received 26th October 2023,
Accepted 19th December 2023

DOI: 10.1039/d3cc05279f

rsc.li/chemcomm

Boosting the effectiveness of UV filters and sunscreen formulations using photostable, non-toxic inorganic platelets†

Lina Chen,‡[a] Junxin Wang,‡[ac] Xuwen Wu,[b] Claire T. Coulthard,[a] Yong Qian,[b] Chunping Chen *[a] and Dermot O'Hare *[a]

We have studied the size-dependent optical scattering of aqueous suspensions containing Mg_2Al-LDH platelets, which exhibit high total- and side-scatterings. By incorporating 3 wt% Mg_2Al-LDH platelets (280 nm) in a commercial sunscreen formulation, we achieved a twofold Sun Protection Factor boost, providing a promising, high-efficient and non-toxic strategy to enhance sunscreen effectiveness.

Overexposure to UV radiation can lead to considerable harm to humans, including sunburn, erythema, premature skin aging, and the risk of skin cancers.[1,2] To safeguard against UV radiation, sunscreens have been developed since 1928. In 2022 the global sun care product market size was valued at $13.97 billion. Projections indicate an anticipated growth from $14.40 billion in 2023 to $19.65 billion by 2030.[3,4] The active ingredient in sunscreen is the UV filter, which can be classified as either physical or chemical UV filters. Typical physical UV filters are inorganic compounds (*e.g.*, TiO_2 and ZnO) which can protect the skin by both reflecting and absorbing the UV radiation. Chemical UV filters are usually organic compounds, such as triazines, avobenzones and ensulizoles, known for their ability to absorb light and release it as heat or light.[5] However, it has recently become evident that both inorganic and organic UV filters have unfavourable safety impacts on both human health and the environment.[6–10] For example, UV absorption by these filters increases their photoactivity, resulting in the generation of harmful radicals.[9,10] A number of commonly used organic UV filters (*e.g.*, ethylhexyl triazone) have been found in several aquatic organisms, raising concerns on their potential environmental impacts.[7] Therefore, a key challenge has arisen in minimising the quantities of UV filters used in sunscreen formulations while still ensuring high sun protection efficacy.

The incorporation of a sun protection factor (SPF) booster into sunscreen formulations has been considered as an effective strategy to reduce the proportion of the active UV filter but still offering a high level of skin protection.[11] SPF boosters do not act as active optical absorbers. Instead, they should meet specific requirements as an ingredient in sunscreen, possessing several key attributes: (i) negligible UV radiation absorption; (ii) safe for both human use and the environment; (iii) compatibility with a wide variety of sunscreen formulations. Significant effort has been focused on the development of SPF boosters from natural sources, such as green coffee oil, spruce bark stilbenes, and lignin-based substances (*e.g.*, lignosulfonates).[12–17] Another type of SPF boosters is synthetic polymer-based materials, such as polydopamines and styrene/acrylates copolymers.[18,19] Some of them have been commercialised. Sunhancer™ (made from plant sources by Lubrizol) and SunSpheres™ (a copolymer from Dow Chemicals) are two examples of SPF boosters in the current market. Although these SPF boosters are biocompatible, they both usually contain organic components with UV absorption. This may lead to poor photostability or require restricted cosmetic application due to the strict audit process concerning both legal and safety use considerations.[20] Some attempts have been made to use inorganic materials as SPF boosters, such as TiO_2, ZnO, silica and alumina. Typically, inorganic materials can enhance the UV absorption efficiency of the organic UV filter. For instance, the incorporation of 10% spherical silica can boost the UV absorbance of Evans blue by a factor of 1.8.[21] However, other potential inorganic boosters (*e.g.*, TiO_2) exhibit photocatalytic activity, which can result in the photodegradation of organic UV filter component or generation of harmful radicals. Some inorganic SPF boosters, such as ZnO and TiO_2, have been

[a] *Chemistry Research Laboratory, Department of Chemistry, University of Oxford, Mansfield Road, Oxford, OX1 3TA, UK. E-mail: chunping.chen@chem.ox.ac.uk, dermot.ohare@chem.ox.ac.uk*
[b] *School of Chemistry and Chemical Engineering, South China University of Technology, 381 Wushan Road, Tianhe District, Guangzhou 510640, China*
[c] *Department of Materials Science and Metallurgy, University of Cambridge, 27 Charles Babbage Road, Cambridge CB3 0FS, UK*

† Electronic supplementary information (ESI) available: Experimental procedures. See DOI: https://doi.org/10.1039/d3cc05279f

‡ Lina Chen and Junxin Wang are co-first author as they contribute equally to this paper.

approved as UV filters, leading to their use as SPF boosters in sunscreen restricted and limited by regulation.[22] Hence, there is an urgent need to develop biocompatible, safe and effective inorganic SPF boosters to enhance both the efficacy and safety of sunscreen formulations.

Layered double hydroxides (LDHs) are a large class of anion exchangeable inorganic materials that are described by the formula $\left[M_{1-x}M'_x(OH)_2\right]^{a+}\left[(A^{n-})_{a/n}\right]\cdot bH_2O$ (M and M′ are divalent and trivalent metal cations respectively, A is charge balancing anion, and $0 < x < 1$). The first naturally occurring LDH was named hydrotalcite, $[Mg_{0.75}Al_{0.25}(OH)_2][CO_3]_{0.125}\cdot 0.5H_2O$. In general, $[Mg_{1-x}Al_x(OH)_2][CO_3]_{x/2}\cdot bH_2O$ (noted as ($Mg_{(1-x)/x}$Al LDHs)) are proven to be biocompatible and non-toxic materials. MgAl-LDHs have been generally recognized as safe (GRAS) by the US Food and Drug Administration (FDA) (UNII:17432CG1KU)[23] and it also has EU approval as an antacid medicine and as a food contact safe material (GRAS) (PM/REF: 34690 & 60080).[24] Additionally, LDHs have been shown to induce low cell cytotoxicity in a number of studies.[25–27] Furthermore, a related zinc layered hydroxide has been commercialised as an active ingredient in a face brightening cosmetic (Vitabrid C$^{12\text{TM}}$).[28] In addition to the known safety data for $Mg_{(1-x)/x}$Al-LDHs, there are potentially significant additional advantages for its use as an effective booster in sunscreen formulations: (i) its white appearance; (ii) thermal and UV stability; and (iii) low photocatalytic activity; (iv) existing commercial good manufacturing practice (GMP) production capacity. In earlier studies, the research mainly focused on the use of LDHs as UV filters by designing and synthesizing molecular UV absorbers intercalated within LDHs structure. However, LDHs in those cases were functioned as UV absorbers rather than SPF boosters.[29] Herein, we have exploited size-dependent particle scattering as a SPF boost mechanism to enhance the optical absorbance of an absorber formulation.[30] Although the scattering of UV radiation by $Mg_{(1-x)/x}$Al-LDH particles has been reported,[31] their use as tailor-made SPF booster to enhance SPF in sunscreen formulations has not been reported.

In this work, we have systematically studied the platelet diameter-dependence of the optical scatterings of Mg_2Al-LDH 2D platelets in aqueous suspensions using an integrating sphere measurement system (Fig. S1, ESI†). We have discovered a size-optimised Mg_2Al-LDH platelet for boosting the UV absorption performance of skin contact approved broad spectrum UV absorbers.

We prepared five Mg_2Al-LDH 2D platelet samples with the platelet diameter distribution covering the range 18–376 nm. To enable platelet diameter control, we created instantaneous nucleation of the Mg_2Al-LDH platelets by rapidly mixing the metal precursors with a mixture of sodium carbonate and sodium hydroxide solution. The as-formed wet solid was then dispersed in deionised (DI) water for subsequent aging process at the various temperatures between 25–200 °C to control the final particle diameters of Mg_2Al-LDH platelets. Mg_2Al-LDHs prepared after aging for 18 h at 25, 50, 100, 150 and 200 °C, are denoted as Mg_2Al-LDH-T (T is the temperature. *e.g.*, Mg_2Al-LDH-150 is the sample that was obtained at 150 °C). Full synthesis details were given in the ESI.† The powder X-ray diffraction (XRD) data for all samples are shown in Fig. 1a. They are typical patterns expected for carbonate intercalated Mg_2Al-LDHs with characteristic Bragg reflections (003), (006), (012), (110) and (113). The relative intensity of (012), (110) and (113) compared to the (003) Bragg reflections decreased with increasing aging temperature during the synthesis. This may be attributed to an increase in the preferred orientation of the larger diameter platelets on the XRD sample plate holder. In addition, the TEM images show that the average particle diameters of Mg_2Al-LDH samples increased with increasing the aging temperature, ranging from 18–376 nm (Fig. 1b–f). The smaller platelets are more uniform in diameter with standard deviations between ±3 and ±19 nm. The nucleation and aging growth mechanism means that the larger diameter platelets exhibit a larger standard deviation, *i.e.* ±55 nm for Mg_2Al-LDH-150.

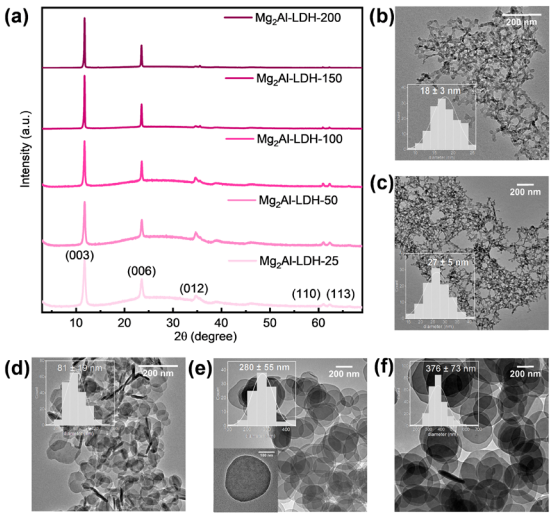

Fig. 1 (a) XRD patterns for Mg_2Al-LDH-T platelets; TEM images for (b) Mg_2Al-LDH-25, (c) Mg_2Al-LDH-50, (d) Mg_2Al-LDH-100, (e) Mg_2Al-LDH-150 and (f) Mg_2Al-LDH-200. Insets are the particle diameter distributions measured from TEM images.

The Mg_2Al-LDH-T platelets all exhibit negligible UV absorption, especially in the UVA and UVB ranges (UVA: 320–400 nm; UVB: 290–320 nm) (Fig. 2a), indicating that Mg_2Al-LDHs have low photoactivity as expected for a material with a quoted optical band gap of 3.12 eV.[32] The UV/vis absorption of Tinosorb®S Lite Aqua (bis-ethylhexyloxyphenol methoxyphenyl triazine and acrylates/C12-22 alkyl methacrylate copolymer), a commercial, skin contact approved broad spectrum UV filter, is shown in Fig. 2b. An aqueous solution containing 0.0003 wt% Tinosorb®S Lite Aqua exhibits a 7.9% UV absorbance at 340 nm. The UV absorbance dramatically increased up to 36.2% after adding 0.1 wt% Mg_2Al-LDH-150 platelets to the Tinosorb®S Lite Aqua solution. The performance of other sized Mg_2Al-LDH-T platelet/Tinosorb®S Lite Aqua suspensions were measured to investigate the particle size dependence on the total optical absorption as shown in Fig. 2c. Fig. 2d summarises

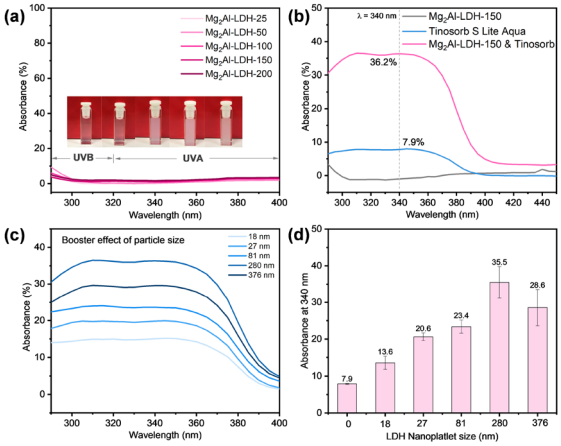

Fig. 2 (a) UV absorbance of Mg_2Al-LDH platelet aqueous dispersions. The inset images are the dispersion of 0.1 wt% Mg_2Al-LDH in DI water, from left to right are Mg_2Al-LDH-25, Mg_2Al-LDH-50, Mg_2Al-LDH-100, Mg_2Al-LDH-150 and Mg_2Al-LDH-200, respectively; (b) boosting the UV absorbance of UV filter Tinosorb S Lite Aqua by Mg_2Al-LDH-150; (c) the boosting effect of LDH platelet sizes on Tinosorb S Lite Aqua and (d) their summary of the absorbance at 340 nm. The loading of all LDHs is fixed at 0.1 wt% and Tinosorb S Lite Aqua at A 0.0003 wt%. Error bar represents the standard error from repeated experiments.

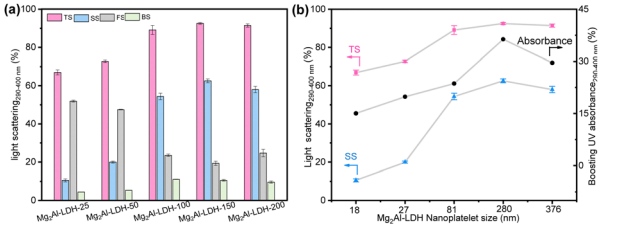

Fig. 3 (a) Mg_2Al-LDH-150 platelet size-dependence light scattering; (b) the comparison of the size-dependence total scattering, side scattering and absorbance to the size-dependence boost effect. Error bar represents the standard error from repeated experiments.

the enhancement of the UV absorbance resulting from the addition of the Mg_2Al-LDH-T platelets, indicating that all Mg_2Al-LDH-T platelets have a positive impact on the overall absorption in the UV range. There is a 1.7-4.5-fold enhancement on the UV absorption of Tinosorb®S Lite Aqua. The greatest enhancement (*ca.* 4.5 times) in the UV absorbance was observed when using Mg_2Al-LDH-150 platelets with an average platelet diameter of 280 nm.

The UV boosting effect of Mg_2Al-LDH-150 platelet loading in 0.003 wt% Tinosorb®S Lite Aqua solution was investigated. The UV spectra (Fig. S2, ESI†) show that the UV absorption increases with an increase in the platelet loading and reaches the highest UV absorbance boosting effect at 0.1 wt% loading. It is even more significant, from a commercial perspective, the boosting effect still has about 3.4 times with less loading (only 0.05 wt%). Other commercial, skin contact-approved UV filters, including UVB filters (Uvinul® T 150: ethylhexyl triazone) and UVA filters (Uvinul® A Plus: diethylamino hydroxybenzoyl hexyl benzoate) were also used in this study. The absorbances of these filters are significantly enhanced by addition of 0.1 wt% Mg_2Al-LDH-150 with a 3.5-fold enhancement at 360 nm for Uvinul® A Plus Granular (Fig. S3a, ESI†) and 3.8-fold enhancement at 310 nm for Uvinul® T 150 (Fig. S3b, ESI†).

The origin of the optical boosting was investigated by performing detailed studies of the optical scatterings (290–400 nm) from aqueous dispersions of the Mg_2Al-LDH-T platelets. The impacts of LDH particle diameter and loading on the light scatterings are shown in Fig. 3 and Fig. S4 (ESI†), respectively. A high total scattering (TS) of up to 92.5% (Fig. 3a) was observed in the dispersions of LDH platelets. Upon increasing the particle diameter, the total scattering increased, reaching a plateau at the particle diameter larger than 280 nm (Mg_2Al-LDH-150). The side scattering (SS) increased with particle diameter from 18 to 280 nm, and then slightly decreased. A slight difference in optical scatterings between Mg_2Al-LDH-150 and Mg_2Al-LDH-200 might be due to a partial overlap in the particle sizes, as also evidenced by a corresponding overlap in the UV boosting effect in Fig. 2d. The highest proportion of side scattering was found to be 63% for the dispersion of Mg_2Al-LDH-150 platelets with the particle diameter of 280 nm. High forward scattering (~50%) was found for smaller particle diameters, whereas low forward scattering (~20%) for larger platelets (Table S1, ESI†). In general, all Mg_2Al-LDH-T samples exhibited very low backward scattering (~10%). The optical scattering dependence on the LDH solid content are shown in Fig. S4 and Table S2 (ESI†). It is surprising to find that, even at a low solid content of 0.03 wt%, the Mg_2Al-LDH-150 platelets still exhibit a high total scattering of up to 81% (Fig. S4a, ESI†). The total scattering increased with increasing the solid content reaching a plateau (~92.5%) when solid content is higher than 0.1 wt%. The highest proportion (63%) of side scattering was observed at a solid content of 0.1 wt%. The low backward scattering was obtained over all solid content fractions studied. The diameter-dependence of both total scattering and side scattering was plotted alongside the diameter-dependence of the boosting effect (Fig. 3b). The data indicates that the boosting effect is strongly correlated to the side scattering of LDH platelets. The same correlation was also found in the solid content data (Fig. S4b, ESI†).

The SPF values of a commercial sunscreen containing 0–7 wt% Mg_2Al-LDH-150 were measured by a specialised UV-2000s ultraviolet transmittance analyser (Labsphere, USA) (Fig. 4). We found that the SPF values of these commercial sunscreen formulations increased with the addition of Mg_2Al-LDH-150 platelets. Promisingly, up to a 2-fold increase in SPF was observed at a Mg_2Al-LDH loading of 3 wt%. This boosting effect (206%) ranks top among the reported SPF boosters as summarized in the Table S3 (ESI†). The stability of 0.1 wt% Mg_2Al-LDH-150 platelets in a sunscreen suspension was studied, revealing that the optical absorbance remained constant after 240 h in the dark (Fig. 4b).

The photostability was also measured by comparing the absorbance of a mixture before and after 2-h UV radiation. A negligible difference was found in the absorbance curves (Fig. S5, ESI†). TEM image confirmed that the morphology of

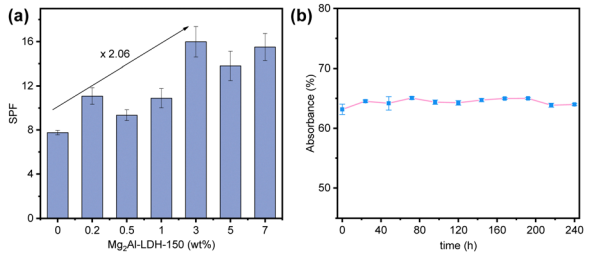

Fig. 4 (a) SPF values of a commercial sunscreen with different loadings of Mg_2Al-LDH-150. (b) The stability of the UV absorbance of commercial sunscreen and 0.1 wt% Mg_2Al-LDH-150 platelet mixture. Error bar represents the standard error from the repeated experiments.

Mg_2Al-LDH-150 remains the same after 2 h UVA radiation (Fig. S6, ESI†). These findings demonstrate that Mg_2Al-LDH platelets have neither chemical nor photo-induced interactions with the sunscreen ingredients that may affect its UV absorbance performance, this will encourage further studies of these materials in commercial UV blocking/cosmetic products.

In summary, size dependent optical scatterings of aqueous dispersions containing Mg_2Al-LDH platelets with diameters ranging from 18 to 376 nm have been studied. These platelets show negligible optical absorbance across the UV/vis spectrum. Instead, they present high total and side scattering. The total scattering/side scattering increases with increasing the particle size and/or loading, reaching maximum when the platelet diameter is 280 nm. We find that the UV absorbance boosting of these platelets is highly correlated to their side scattering performance. The Mg_2Al-LDH-150 sample (280 nm at 0.1 wt%) produces the largest boost (3.5–4.5-fold) in the UVA and UVB absorbance when mixed with widely used, commercial sunscreen adsorbers. In a commercial sunscreen, the SPF can be boosted by 2.06-fold using Mg_2Al-LDH-150. These biocompatible, non-toxic, safe, and effective LDH platelets provide a promising option for boosting the effectiveness of UV filter formulations.

Lina Chen and Junxin Wang performed the synthetic and experimental work; Claire T. Coulthard assisted with the electron microscopy studies; Xuwen Wu and Yong Qian conducted the SPF measurement; Chunping Chen supervised the work; and Dermot O'Hare conceptualised the research and acquired funding.

J. Wang, L. Chen, C. Chen would like to thank SCG Chemicals Public Co., Ltd. (Thailand) for funding. J. Wang acknowledges financial support from European Union's Horizon 2020 Marie Skłodowska-Curie Actions under grant agreement number 892131-PLECTRA-H2020-MSCA-IF-2019.

Conflicts of interest

The authors declare no competing financial interests.

Notes and references

1 R. M. Lucas, S. Yazar, A. R. Young, M. Norval, F. R. de Gruijl, Y. Takizawa, L. E. Rhodes, C. A. Sinclair and R. E. Neale, *Photoch. Photobio. Sci.*, 2019, **18**, 641–680.
2 F. R. de Gruijl, *Exp. Dermatol.*, 2017, **26**, 557–562.
3 D. R. Sambandan and D. Ratner, *J. Am. Acad. Dermatol.*, 2011, **64**, 748–758.
4 U. Osterwalder, M. Sohn and B. Herzog, *Photodermatol. Photoimmunol. Photomed.*, 2014, **30**, 62–80.
5 F. R. de Gruijl, *Eur. J. Cancer*, 1999, **35**, 2003–2009.
6 M. Krause, A. Klit, M. Blomberg Jensen, T. Søeborg, H. Frederiksen, M. Schlumpf, W. Lichtensteiger, N. E. Skakkebaek and K. T. Drzewiecki, *Int. J. Androl.*, 2012, **35**, 424–436.
7 M. I. Cadena-Aizaga, S. Montesdeoca-Esponda, M. E. Torres-Padrón, Z. Sosa-Ferrera and J. J. Santana-Rodríguez, *Trends Environ. Anal. Chem.*, 2020, **25**, e00079.
8 A. S. Barnard, *Nat. Nanotechnol.*, 2010, **5**, 271–274.
9 K. M. Hanson, E. Gratton and C. J. Bardeen, *Free Radical Biol. Med.*, 2006, **41**, 1205–1212.
10 Z. Pan, W. Lee, L. Slutsky, R. A. F. Clark, N. Pernodet and M. H. Rafailovich, *Small*, 2009, **5**, 511–520.
11 M. Sohn, in *Principles and Practice of Photoprotection*, ed. S. Q. Wang and H. W. Lim, Springer International Publishing, Cham, 2016, pp. 227–245.
12 B. G. Chiari, E. Trovatti, É. Pecoraro, M. A. Corrêa, R. M. B. Cicarelli, S. J. L. Ribeiro and V. L. B. Isaac, *Ind. Crops Prod.*, 2014, **52**, 389–393.
13 J. Dou, M. Sui, K. Malinen, T. Pesonen, T. Isohanni and T. Vuorinen, *Green Chem.*, 2022, **24**, 2962–2974.
14 H. Sadeghifar and A. Ragauskas, *Polymers*, 2020, **12**, 1134.
15 F. Lorquin, J. Lorquin, M. Claeys-Bruno, M. Rollet, M. Robin, C. Di Giorgio and P. Piccerelle, *Sustainable Chem. Pharm.*, 2021, **24**, 100539.
16 Y. Qian, X. Qiu and S. Zhu, *Green Chem.*, 2015, **17**, 320–324.
17 Y. Wu, X. Wu, A. Zhang, X. Ouyang, H. Lou, D. Yang, Y. Qian and X. Qiu, *Adv. Funct. Mater.*, 2023, **33**, 2303889.
18 Y. Wongngam, G. Supanakorn, R. Thiramanas and D. Polpanich, *ACS Biomater. Sci. Eng.*, 2021, **7**, 3114–3122.
19 T. Martin and T. Burns, *Novel graft polymer boosts SPF performance*, 2006.
20 S. Nanda, A. Nanda, S. Lohan, R. Kaur and B. Singh, in *Nanobiomaterials in Galenic Formulations and Cosmetics*, ed. A. M. Grumezescu, William Andrew Publishing, 2016, pp. 47–67.
21 J. Lademann, S. Schanzer, U. Jacobi, H. Schaefer, F. Pflücker, H. Driller, J. Beck, M. Meinke, A. Roggan and W. Sterry, *J. biomedi. opt.*, 2005, **10**, 014008.
22 O. P. Egambaram, S. Kesavan Pillai and S. S. Ray, *Photochem. Photobiol.*, 2020, **96**, 779–797.
23 US FDA registration as GRAS (UNII: 17432CG1KU, **https://drugs.ncats.io/drug/17432CG1KU**).
24 EU Approval for Food Contact. PM/REF: 34690 & 60080 (**https://www.legislation.gov.uk/uksi/2006/1401/pdfs/uksi_20061401_en.pdf**).
25 T. Hu, Z. Gu, G. R. Williams, M. Strimaite, J. Zha, Z. Zhou, X. Zhang, C. Tan and R. Liang, *Chem. Soc. Rev.*, 2022, **51**, 6126–6176.
26 T. Yamaguchi, H.-M. Kim, B. C. Jung, Y. S. Kim and J.-M. Oh, *Appl. Clay Sci.*, 2022, **225**, 106549.
27 C. Chen, L. K. Yee, H. Gong, Y. Zhang and R. Xu, *Nanoscale*, 2013, **5**, 4314–4320.
28 Vitabrid C^{12} face brightening powder (**https://vitabrid.ee/en/face-brightening-powder/**).
29 W. K. Ng'etich and B. S. Martincigh, *Appl. Clay Sci.*, 2021, **208**, 106095.
30 T. A. D. Silva, T. G. D. Nascimento, R. E. Yatsuzuka, L. A. M. Grillo and C. B. Dornelas, *Einstein (Sao Paulo)*, 2019, **17**, 1–6.
31 W. Shi, Y. Lin, S. Zhang, R. Tian, R. Liang, M. Wei, D. G. Evans and X. Duan, *Phys. Chem. Chem. Phys.*, 2013, **15**, 18217–18222.
32 B. R. Gevers, E. Roduner and F. J. W. J. Labuschagné, *Mater. Adv.*, 2022, **3**, 962–977.

